

Development and Evaluation of High-Resolution Climate Simulations over the Mountainous Northeastern United States

JONATHAN M. WINTER

Department of Geography, and Department of Earth Sciences, Dartmouth College, Hanover, New Hampshire

BRIAN BECKAGE AND GABRIELA BUCINI

Department of Plant Biology, University of Vermont, Burlington, Vermont

RADLEY M. HORTON

Columbia University, NASA Goddard Institute for Space Studies, New York, New York

PATRICK J. CLEMINS

Department of Computer Science, University of Vermont, Burlington, Vermont

(Manuscript received 3 April 2015, in final form 3 November 2015)

ABSTRACT

The mountain regions of the northeastern United States are a critical socioeconomic resource for Vermont, New York State, New Hampshire, Maine, and southern Quebec. While global climate models (GCMs) are important tools for climate change risk assessment at regional scales, even the increased spatial resolution of statistically downscaled GCMs (commonly $\sim 1/8^\circ$) is not sufficient for hydrologic, ecologic, and land-use modeling of small watersheds within the mountainous Northeast. To address this limitation, an ensemble of topographically downscaled, high-resolution ($30''$), daily 2-m maximum air temperature; 2-m minimum air temperature; and precipitation simulations are developed for the mountainous Northeast by applying an additional level of downscaling to intermediately downscaled ($1/8^\circ$) data using high-resolution topography and station observations. First, observed relationships between 2-m air temperature and elevation and between precipitation and elevation are derived. Then, these relationships are combined with spatial interpolation to enhance the resolution of intermediately downscaled GCM simulations. The resulting topographically downscaled dataset is analyzed for its ability to reproduce station observations. Topographic downscaling adds value to intermediately downscaled maximum and minimum 2-m air temperature at high-elevation stations, as well as moderately improves domain-averaged maximum and minimum 2-m air temperature. Topographic downscaling also improves mean precipitation but not daily probability distributions of precipitation. Overall, the utility of topographic downscaling is dependent on the initial bias of the intermediately downscaled product and the magnitude of the elevation adjustment. As the initial bias or elevation adjustment increases, more value is added to the topographically downscaled product.

1. Introduction

Global climate models (GCMs) are essential for projecting future climate; however, despite the rapid advance in their ability to simulate the climate system at increasing spatial resolutions, GCMs cannot capture well local and

regional ($<10^2$ km) climate features (Taylor et al. 2012). For example, where elevation and land–water boundaries vary on the scale of 10^0 – 10^2 km, hydrological and ecological impacts modeling will benefit from high-resolution climate data. There have been a variety of efforts to bridge this gap in resolution, broadly referred to as downscaling, that generally fall into one of two categories, dynamical (Mearns et al. 2009; Giorgi et al. 2009; van der Linden and Mitchell 2009) or statistical (Wilby et al. 1998; Maurer and Hidalgo 2008; Ahmed et al. 2013; Brekke et al. 2013).

Corresponding author address: Jonathan M. Winter, Department of Geography, Department of Earth Sciences, Dartmouth College, 6017 Fairchild Hall, Hanover, NH 03755.
E-mail: jwinter@dartmouth.edu

Statistically downscaled GCM projections have been used for a variety of applications, including water resources and hydrology (Wood et al. 2004; Rajagopal et al. 2014), surface (2-m air) temperature (Pierce et al. 2013), human health (Petkova et al. 2013), extreme precipitation events (Norton et al. 2011; Sunyer et al. 2012), wildfire (Westerling and Bryant 2008; Abatzoglou and Brown 2012), agriculture (Islam et al. 2012; Rosenzweig et al. 2014), and snowfall (Huntington and Niswonger 2012; Guilbert et al. 2014). Typically, the spatial resolution of statistically downscaled products is constrained by the need for a gridded target observational dataset at that resolution. Over the contiguous United States, high-resolution gridded observations are available at $1/8^\circ$ (~ 12 km), with the most recent datasets extending to $1/16^\circ$ (Maurer et al. 2002; Livneh et al. 2013).

While the utility of statistically downscaled data at $1/8^\circ$, hereafter referred to as intermediately downscaled, in climate change impacts and adaptation analyses is clear, highly tailored and parameterized climate impacts models (e.g., hydrologic, ecosystem, crop, and land use) are increasingly able to ingest and utilize finer-scale data. Intermediately downscaled projections have a significantly improved spatial resolution relative to the GCMs from which they originate. Nevertheless, their coarse resolution compared to impacts models poses an obstacle to accurate projections of hydrologic, ecosystem, etc. dynamics determined by variability in climate occurring at sub- $1/8^\circ$ spatial scales.

Four methods of creating climate change projections at higher spatial resolution than typical downscaled products ($1/8^\circ$), hereafter referred to as high resolution, are dynamical downscaling, interpolation, stochastic weather generation, and empirical climate relationships.

Many regional climate models (RCMs) now have nonhydrostatic cores, eliminating the hydrostatic limitation in spatial resolution of approximately 10 km (Dudhia 1993). However, running an RCM at a resolution of 10 km or higher over long time periods is extremely computationally intensive. Further, the setup of such high-resolution simulations raises a number of unique issues associated with the need for multiple nested model runs, very small time steps, and parameterization. For these reasons, RCMs are not typically run at very high (e.g., $30''$ or approximately 1 km) resolution.

Interpolation relies on simple horizontal distances or, in more sophisticated implementations, classification and relationships between stations. For example, Hijmans et al. (2005) used a thin-plate smoothing spline algorithm to interpolate station data to $30''$ resolution using latitude, longitude, and elevation as independent

variables. Additional climatological interpolation techniques are reviewed in Hartkamp et al. (1999).

Stochastic weather generators can be set to any arbitrary resolution, although the output will be constrained by the resolution of the source data (e.g., observations and GCM simulations) and a variety of issues must be carefully considered to preserve the spatial and temporal coherence of climate (e.g., surface temperature, precipitation, humidity) signals.

Empirical climate relationships use high-resolution data that have a physically based statistical relationship to climate, typically topography, slope, aspect, or some combination of the three. Daly et al. (2000) developed the Parameter-Elevation Regressions on Independent Slopes Model (PRISM), which linearly adjusts climatic variables using a digital elevation model (DEM), and adds weighting information from terrain aspect, coastal proximity, and deviation in the height relative to smoothed topography to create a $2.5'$ time series of monthly maximum surface temperature, minimum surface temperature, and precipitation. Variants of this methodology have been used to produce a number of high-resolution climatic datasets (PRISM Climate Group 2014). Liston and Elder (2006) developed a meteorological model that uses empirical relationships between elevation and precipitation and between elevation and surface temperature to produce uniform, high-resolution atmospheric forcings for terrestrial simulations. Liston and Elder (2006) also use elevation to adjust vapor pressure, and slope and curvature of topography to adjust wind speed and direction.

Our objective was to create a $30''$ (~ 1 km) dataset of daily maximum surface temperature, minimum surface temperature, and precipitation for the Lake Champlain basin to aid in hydrological and ecological modeling of potential climate impacts. Specifically, we develop and evaluate an empirical method to calculate the relationships between elevation and daily maximum surface temperature, daily minimum surface temperature, and precipitation over the region from station data, and then use those relationships to downscale the $1/8^\circ$ bias correction with constructed analogs (BCCA) dataset (Brekke et al. 2013), creating a daily, $30''$ time series for 1970–99.

2. Methodology

a. Study region

We conduct our analysis in the mountainous Northeast, a region that includes northern Vermont, northeastern New York State, northern New Hampshire, southwestern Maine, and southern Canada

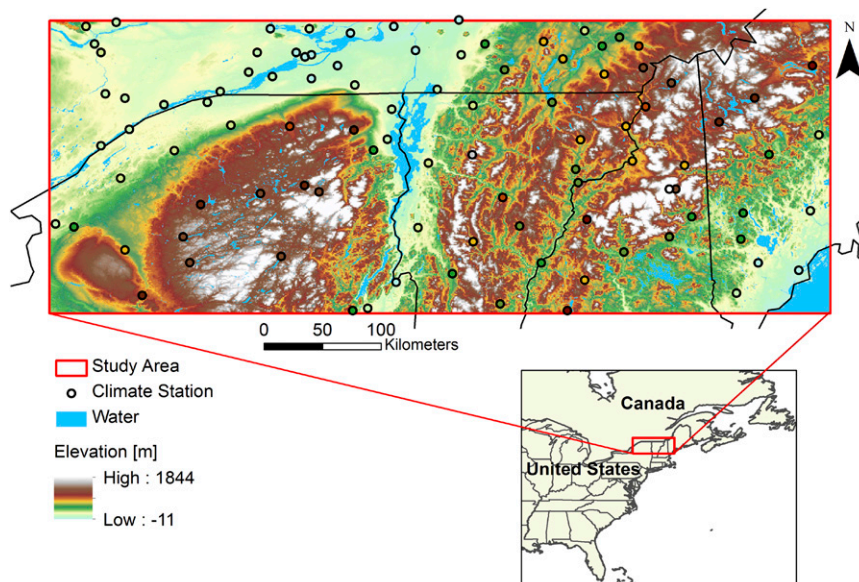


FIG. 1. Downscaling domain topography from 30'' DEM and climate station locations color-coded by station elevation. The study area contains 98 stations that were selected based on coverage for 1970–99 with no more than 20% missing values.

(Fig. 1). Within our study area there are four watersheds of interest that drain into Lake Champlain: Lake Champlain, Missisquoi, Lamoille, and Winooski. The primary topographic features within this domain are the Green Mountains, running through central Vermont; the Adirondack Mountains, clustered in northeastern New York; and the White Mountains, spanning northern New Hampshire and western Maine. Elevations range from 30 to 1340 m MSL.

b. Climate data

Relationships between surface temperature (maximum and minimum) and elevation and between precipitation and elevation were derived from Global Historical Climatology Network (GHCN)-Daily (Menne et al. 2012) station observations. Data were downloaded from NOAA's National Climatic Data Center (NCDC; <http://www.ncdc.noaa.gov/>) and contain daily measurements covering different periods between the early 1900s and 2012. To maximize the number and quality of observed data for analysis, we used stations within and near the Lake Champlain basin that had daily observations for a subset of BCCA temporal coverage, 1970–99, with no more than 20% missing values. The 98 stations selected (Fig. 1) were used for GCM selection, elevation adjustment calculations, and analysis of the topographically downscaled product.

Six simulations from phase 5 of the Coupled Model Intercomparison Project (CMIP5) multimodel ensemble

downscaled to an intermediate resolution ($1/8^\circ$) using BCCA (Brekke et al. 2013) were selected as source data for topographic downscaling to high resolution (30''). BCCA leverages observed climate data to both bias-correct and statistically downscale GCM data; a full description of BCCA methodology can be found in Hidalgo et al. (2008), Maurer and Hidalgo (2008), and Maurer et al. (2010). BCCA has a variety of attributes that make it uniquely suited to evaluate climate change over the Lake Champlain basin. BCCA is a daily product with coverage of both the United States and southern Canada, which is a requirement for use in hydrologic applications in the Lake Champlain basin. In addition, the BCCA ensemble is comprehensive. It includes a total of nine GCMs run as part of phase 3 of the Coupled Model Intercomparison Project (CMIP3) under two Special Report on Emissions Scenarios (SRES) emissions scenarios (Nakićenović and Swart 2000) and 20 GCMs run as part of CMIP5 under two representative concentration pathways (RCPs; Moss et al. 2010). BCCA has been previously used in the Northeast to assess climate change (Ahmed et al. 2013; Guilbert et al. 2014). Ahmed et al. (2013) explore changes in total number of days with more than 10 mm for one GCM and SRES scenario by midcentury, finding that BCCA predicts a relatively small change in days with more than 10 mm relative to other statistical downscaling methods across the Northeast by midcentury. Guilbert et al. (2014) used BCCA data from four GCMs and two RCPs, showing increases in temperature of

approximately 4.5°C and increases in precipitation of approximately 0.3 mm day⁻¹ in the Lake Champlain basin by the end of the century. Guilbert et al. (2014) also explored climate change impacts on high-elevation snowfall, finding an approximate 50% decrease in annual snowfall at six major ski resorts in the Northeast by the end of the century.

CMIP5 BCCA ensemble members, differentiated by source GCM, were selected based on their ability to accurately reproduce station observations over 1970–99. The BCCA datasets were bias corrected using a gridded observational dataset over the period 1950–99, so comparing long-term surface temperature and precipitation averages of BCCA ensemble members is not a useful metric for discerning accuracy across GCMs. Instead, we examine the overlap of the probability distribution for daily surface temperature and precipitation using a skill score defined in section 2d. We used this metric to select the three most accurate CMIP5 BCCA ensemble members for average surface temperature—L’Institut Pierre-Simon Laplace Coupled Model, version 5A, low resolution (IPSL-CM5A-LR); the Norwegian Climate Centre’s Norwegian Earth System Model, version 1 (intermediate resolution) (NorESM1-M); and the Commonwealth Scientific and Industrial Research Organisation and Bureau of Meteorology’s Australian Community Climate and Earth-System Simulator, version 1.0 (ACCESS1.0)—and precipitation—Max Planck Institute Earth System Model, low resolution (MPI-ESM-LR); NorESM1-M; and Geophysical Fluid Dynamics Laboratory Climate Model, version 3 (GFDL CM3). Models were selected based on mean surface temperature, calculated as the average of maximum and minimum surface temperature, to ensure a physically consistent set of models for both maximum and minimum surface temperatures.

c. High-resolution downscaling

The process used to topographically downscale three BCCA ensemble members of maximum surface temperature, minimum surface temperature, and precipitation over the study area for 1970–99 consisted of three basic steps. First, empirical relationships between surface temperature and elevation and between precipitation and elevation were derived. Second, the 1/8° intermediately downscaled GCM simulations were adjusted to a reference elevation (200 m MSL) using the derived relationships and a 1/8° DEM, then interpolated to a grid with the resolution of 30". Third, the 30" interpolated data were topographically adjusted using the derived relationships and a 30" DEM.

1) ELEVATION ADJUSTMENT DERIVATION

Accurately defining the empirical relationships between surface temperature and elevation (i.e., lapse rate) and between precipitation and elevation across the Lake Champlain basin is a critical component of this downscaling approach. To derive these relationships, we leverage the dense meteorological station network of the mountainous Northeast. While we could have also used a gridded 1/8° dataset to derive these relationships, it is possible that the averaging and interpolation used to produce the gridded dataset could change or obfuscate the surface temperature–elevation and precipitation–elevation relationships. Further, the meteorological stations in the mountainous Northeast are well distributed throughout the domain and include a range of elevations (Fig. 1). We used long-term averages of daily data to reduce noise in the presentation of surface temperature and precipitation elevation adjustment estimation; however, the values of elevation adjustments found were confirmed to be identical for daily, monthly, annual, and long-term averaged data.

For maximum and minimum surface temperature, we calculated elevation adjustments that assume a linear relationship between surface temperature and elevation, equivalent to deriving the lapse rate. This assumed form of the temperature–elevation relationship is used widely, including in downscaling applications (Daly et al. 2000; Liston and Elder 2006). We found a significant relationship between surface temperature and latitude; however, there was no clear relationship between surface temperature and longitude over the study area. To account for the effect of latitude on the temperature elevation adjustment, we ran a multiple linear regression of the form:

$$T_{\text{sta}} = T_o - \beta\phi_{\text{sta}} - \gamma z_{\text{sta}},$$

where T_{sta} (°C) is the station surface temperature, T_o (°C) is the y intercept, z_{sta} (m) is the station elevation, ϕ_{sta} (°) is the latitude of the station, γ (°C m⁻¹) is the elevation adjustment, and β [°C (°)⁻¹] is the latitude adjustment. We find γ and β by regressing station long-term averaged daily surface temperatures 1970–99 versus elevation and latitude. The maximum daily surface temperature regression is shown in Fig. 2a. Both γ and β are defined as positive when temperature decreases with increasing elevation and latitude, respectively. The values calculated for the maximum and minimum surface temperature elevation adjustments were 5.92° and 4.85°C km⁻¹, respectively, which are broadly consistent with both the canonical environmental lapse rate of 6°C km⁻¹ (Barry 2008) and more sophisticated

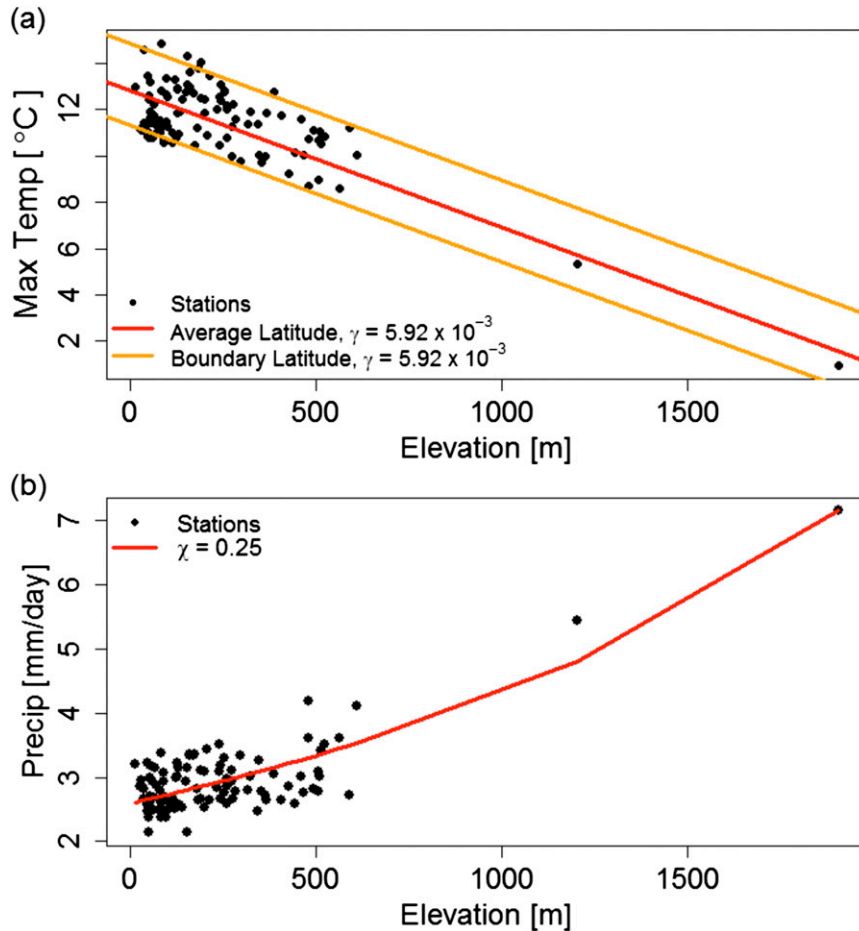


FIG. 2. Derivation of elevation adjustments for (a) max surface temperature, with upper and lower yellow lines depicting the southern and northern boundary latitudes, respectively, and (b) precipitation.

calculations of lapse rates over space and time (Rolland 2003; Liston and Elder 2006; Blandford et al. 2008; Barry 2008).

For precipitation, we calculated an elevation adjustment that assumed a nonlinear functional form based on normalized differences, consistent with Liston and Elder (2006) and Thornton et al. (1997):

$$P_{sta} = P_{ref} \left[\frac{1 + \chi(z_{sta} - z_{ref})}{1 - \chi(z_{sta} - z_{ref})} \right],$$

where P_{sta} (mm day^{-1}) is the station precipitation, P_{ref} (mm day^{-1}) is the expected precipitation at the reference elevation across all stations in the domain, z_{sta} (m) is the station elevation, z_{ref} (m) is the reference elevation, and χ (m^{-1}) is the elevation adjustment. We find χ and P_{ref} by fitting long-term averaged daily station precipitation data to the function above using maximum

likelihood estimation (Fig. 2b). In this case, χ is defined as positive when precipitation increases with increasing elevation. We chose a reference elevation of 200 m MSL based on the domain average station elevation mean (230 m MSL) and median (161 m MSL). The value calculated for the precipitation elevation adjustment was 0.250 km^{-1} . This value is consistent with the range of the elevation adjustment time series constructed by Thornton et al. (1997), despite the fact that Thornton et al. (1997) focused on the Pacific Northwest and limited their derivation of the elevation adjustment to complex terrain.

2) INTERPOLATION

Once the $1/8^\circ$ intermediate-resolution values are translated to a reference elevation using the elevation adjustments described above and a DEM aggregated to $1/8^\circ$, they are then interpolated to a $30''$ high-resolution grid before final modification using a $30''$ DEM and the

elevation adjustments. A variety of methods exist for spatial interpolation (Li and Heap 2014). We chose inverse distance weighting (IDW) interpolation because of its relative simplicity, extensive use in climate applications, and computational efficiency. The high-resolution value (e.g., precipitation and surface temperature) is calculated using intermediate-resolution grid cells weighted by an inverse power of distance:

$$V_i = \frac{\sum_{j=1}^n V_j / D_{ij}^p}{\sum_{j=1}^n 1 / D_{ij}^p},$$

where V_i is the value (e.g., precipitation and surface temperature) at high-resolution grid cell i , V_j is the value at an intermediate-resolution grid cell j , D_{ij} is the distance between the coarse-resolution cell center j and the high-resolution cell center i , p is IDW power, and n is the number of nearest-neighbor intermediate grid cells contributing to the average. The value of p controls the region of influence of each of the coarse cells. As p increases, the region of influence decreases.

IDW interpolation requires two user-defined inputs: the weighting power and the number of neighbors. We ran a sensitivity analysis to find an optimal value for both the weighting power and number of neighbors with the objective to include information at a distance that matches the scale of variation in the climate data (not shown). By matching the scale of variation in the climate data, we avoid oversmoothing the surface (too many neighbors) and introducing unrealistic details or artifacts (too few neighbors). Based on this analysis and exploring the sensitivity of IDW interpolation to a range of values for weighting power and number of neighbors, we chose values of 2 and 9 (3×3), respectively, which maintain patterns in the original coarse surface temperature and precipitation images while creating spatially smooth data (Fig. 3). Our weighting power is consistent with previous climate applications (Lloyd 2005). Because of the high degree of flexibility required for our interpolation process, we coded our own IDW interpolation function in R. We reproduced the results of the IDW interpolation function contained in the R package “gstat” (<https://r-forge.r-project.org/projects/gstat/>) under several test cases to confirm the accuracy of our interpolation function.

3) DOWNSCALING METHODOLOGY

We downscale BCCA using the calculated precipitation and surface temperature elevation adjustments, a high-resolution DEM, and IDW interpolation as follows.

First, precipitation and surface temperature values of each intermediate-resolution cell are translated to the reference elevation of 200 m MSL by applying the functions below. For surface temperature,

$$T_{\text{ref}} = T_{\text{int}} - \gamma(z_{\text{ref}} - z_{\text{int}}),$$

where T_{ref} ($^{\circ}\text{C}$) is the surface temperature at reference elevation z_{ref} (m), T_{int} ($^{\circ}\text{C}$) is the intermediately downscaled surface temperature at elevation z_{int} (m), and γ ($^{\circ}\text{C m}^{-1}$) is the surface temperature adjustment. For precipitation (Liston and Elder 2006),

$$P_{\text{ref}} = P_{\text{int}} \left[\frac{1 + \chi(z_{\text{ref}} - z_{\text{int}})}{1 - \chi(z_{\text{ref}} - z_{\text{int}})} \right],$$

where P_{ref} (mm day^{-1}) is the precipitation at reference elevation z_{ref} (m), P_{int} (mm day^{-1}) is intermediately downscaled precipitation at elevation z_{int} (m), and χ (m^{-1}) is the precipitation elevation adjustment.

Second, T_{ref} and P_{ref} are spatially interpolated from the coarse to the fine grid using IDW. Based on an analysis of spatial climate variability in the intermediate-resolution data, we assign a weighting power of 2 and number of neighbors of 9.

Finally, spatially interpolated surface temperature and precipitation values at the reference elevation are translated to their actual elevation using the derived elevation adjustments and a high-resolution DEM, creating a daily, 30" surface temperature and precipitation dataset. For surface temperature,

$$T_{\text{high}_{\text{tar}}} = T_{\text{high}_{\text{ref}}} - \gamma(z_{\text{tar}} - z_{\text{ref}}),$$

where $T_{\text{high}_{\text{tar}}}$ ($^{\circ}\text{C}$) is the high-resolution surface temperature at the target elevation z_{tar} , $T_{\text{high}_{\text{ref}}}$ ($^{\circ}\text{C}$) is the high-resolution (spatially interpolated) surface temperature at reference elevation z_{ref} (m), and γ ($^{\circ}\text{C m}^{-1}$) is the surface temperature adjustment. For precipitation (Liston and Elder 2006),

$$P_{\text{high}_{\text{tar}}} = P_{\text{high}_{\text{ref}}} \left[\frac{1 + \chi(z_{\text{tar}} - z_{\text{ref}})}{1 - \chi(z_{\text{tar}} - z_{\text{ref}})} \right],$$

where $P_{\text{high}_{\text{tar}}}$ (mm day^{-1}) is the high-resolution precipitation at target elevation z_{tar} (m), $P_{\text{high}_{\text{ref}}}$ (mm day^{-1}) is the high-resolution (spatially interpolated) precipitation at reference elevation z_{ref} (m), and χ (m^{-1}) is the precipitation elevation adjustment.

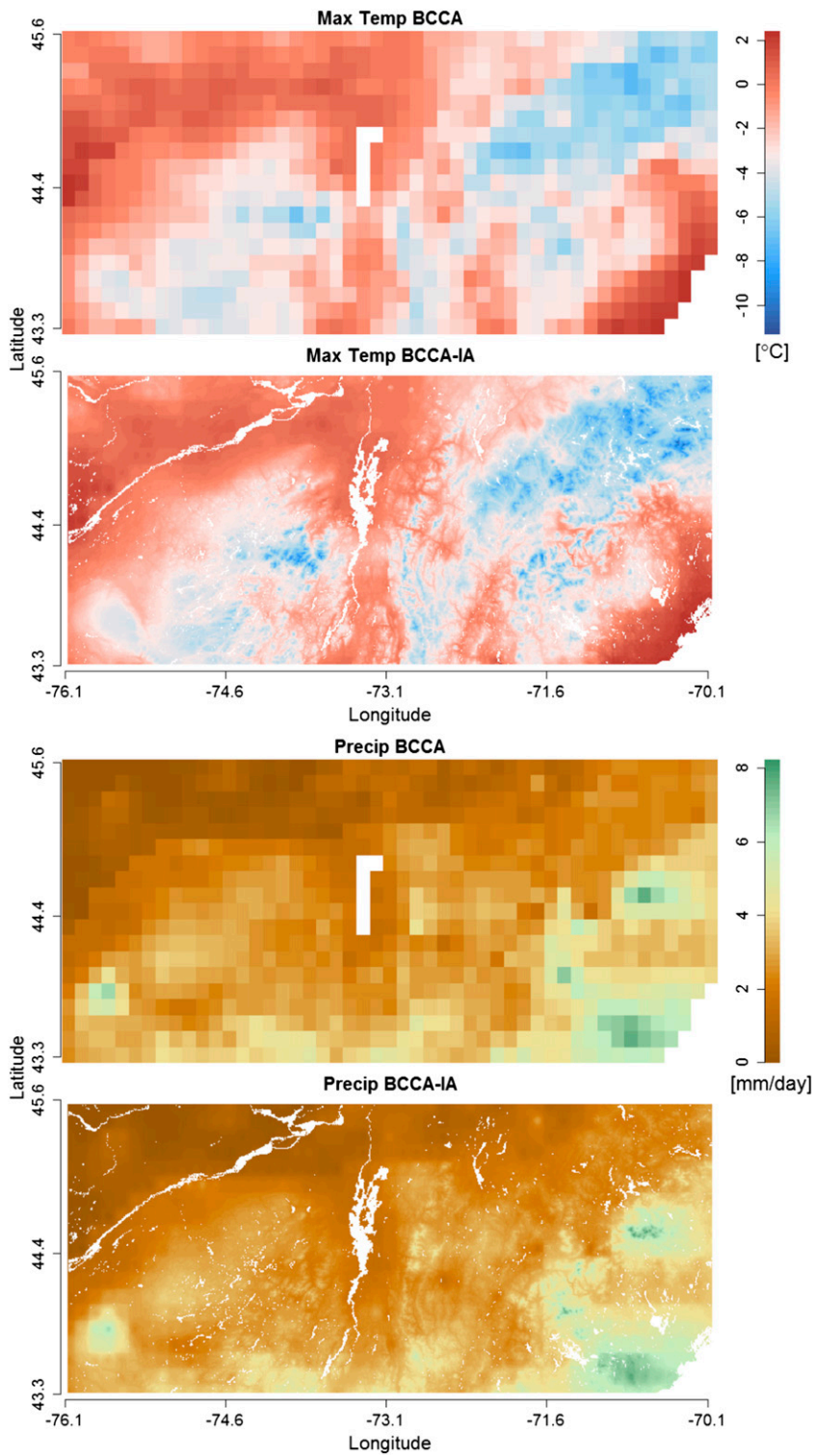


FIG. 3. Example climate data: BCCA and topographically downscaled BCCA (BCCA-IA) for (top) IPSL-CM5A-LR max surface temperature and (bottom) MPI-ESM-LR precipitation on 17 Jan 1970.

d. Topographically downscaled climate data evaluation

We evaluate our developed product by comparing BCCA interpolated and elevation adjusted (BCCA-IA), BCCA interpolated using IDW (BCCA-I), and BCCA to station observations from 1970 to 1999. Daily data, as opposed to monthly or annual, is of critical importance for a variety of impacts assessments (heat waves, floods, growing season length, etc.). We therefore focus our analysis on the daily time scale. BCCA-I is simply an interpolated version of BCCA and does not include any explicit elevation adjustments. In the context of this study it serves as a reference high-resolution dataset with no additional information. Specifically, it describes a simple method that could be used for downscaling $1/8^\circ$ climate data to $30''$ without topographic information or relationships between surface temperature and elevation and precipitation and elevation. Because the interpolation is not done at the reference elevation, it should not be considered an intermediate step between BCCA and BCCA-IA.

We rely on three metrics to assess BCCA, BCCA-I, and BCCA-IA against station observations. The first is simply the absolute value of the bias, calculated as the absolute value of the long-term mean of each daily climate product (i.e., BCCA, BCCA-I, and BCCA-IA) minus the long-term mean of daily observed data. We present this metric by station and averaged across all stations in the domain. The change in absolute bias between BCCA, BCCA-I, and BCCA-IA is assessed relative to the absolute bias spread across the BCCA ensemble.

The second metric we use to evaluate the climate datasets is the skill score S_{score} of Perkins et al. (2007). The Perkins et al. (2007) skill score is an intuitive measure of the overlap between two probability distributions and is calculated using the following equation:

$$S_{\text{score}} = \sum_{i=1}^n \min(Z_m - Z_o),$$

where n is the number of bins in the probability distribution, Z_m is the model frequency of values for bin i , and Z_o is the observed frequency of values for bin i (Perkins et al. 2007). An S_{score} close to zero denotes a poor simulation (nonoverlapping probability distributions), and an S_{score} close to one denotes an accurate simulation (overlapping probability distributions). This measure is uniquely suited for assessing daily temperature and precipitation data and is a more rigorous standard than assessing statistical moments such as mean and variance.

As in Perkins et al. (2007), we use a binning interval of 1 mm day^{-1} for precipitation and 0.5°C for maximum and minimum surface temperature. We use 0.03 as a significant difference in S_{score} based on a sensitivity test of the skill score to sampling conducted by Perkins et al. (2007) in which 100 partial probability distributions were obtained by randomly sampling 75% of a full probability distribution. The lowest partial probability distribution S_{score} found was 0.97; thus, the greatest difference between the partial and full probability distributions and perfect overlap was 0.03 (Perkins et al. 2007). In addition to this threshold, we also consider the spread of S_{score} values across the BCCA ensemble members to determine value added by the elevation adjustments.

The third metric we use to assess our topographically downscaled product is root-mean-square deviation (RMSD). To calculate this measure, the simulated and observed daily time series of surface temperature and precipitation are first ranked from lowest value to highest value, as GCMs are not expected to simulate shorter-term sequencing of climatic events (i.e., a GCM should capture the frequency and magnitude of heavy precipitation events, but is not expected to place those events in the correct calendar years). Once rank ordered, the RMSD is calculated using the following equation:

$$\text{RMSD} = \sqrt{\sum_{i=1}^n (X_m - X_o)^2},$$

where n is the length of the data series, X_m is the model value for ranked index i , and X_o is the observed value for ranked index i . Opposite of S_{score} , low values of RMSD demonstrate skill in simulation, with the ideal RMSD value (i.e., perfect matching of the two ranked series) being zero. To assess the value added by elevation adjustments using RMSD, we compare changes in RMSD to the spread of RMSD values across the BCCA ensemble members.

3. Results and discussion

First, we explore topographic downscaling at the station level, presenting long-term averages and histograms of station observations, gridded observations, BCCA, BCCA-I, and BCCA-IA at two stations differentiated by elevation: Burlington, Vermont (101 m), and Mt. Mansfield, Vermont (1204 m). Next, we assess the performance of BCCA, BCCA-I, and BCCA-IA for all stations within the domain in the context of elevation using S_{score} and RMSD. Finally, we average the absolute value of the bias, S_{score} , and RMSD for all stations within the domain to evaluate the aggregate

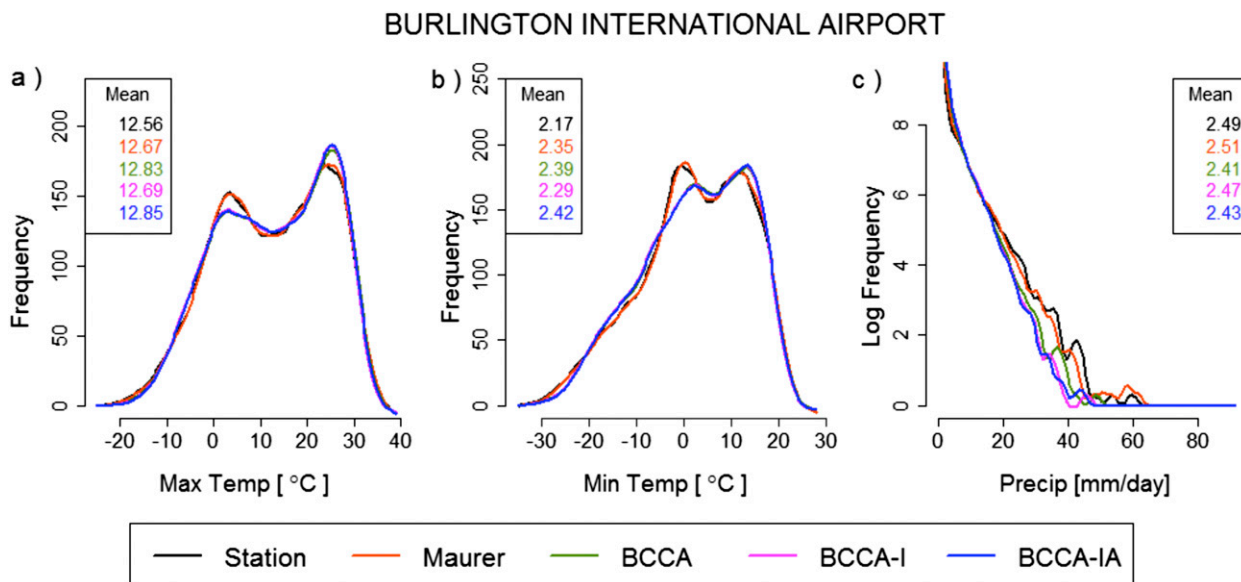


FIG. 4. Daily histograms for Burlington station 1970–99: (a) max surface temperature from station observations, Maurer observations ($1/8^\circ$), IPSL-CM5A-LR BCCA ($1/8^\circ$), IPSL-CM5A-LR BCCA-I ($30''$), and IPSL-CM5A-LR BCCA-IA ($30''$); (b) min surface temperature from station observations, Maurer observations ($1/8^\circ$), IPSL-CM5A-LR BCCA ($1/8^\circ$), IPSL-CM5A-LR BCCA-I ($30''$), and IPSL-CM5A-LR BCCA-IA ($30''$); and (c) precipitation from station observations, Maurer observations ($1/8^\circ$), MPI-ESM-LR BCCA ($1/8^\circ$), MPI-ESM-LR BCCA-I ($30''$), and MPI-ESM-LR BCCA-IA ($30''$). Numbers in legend are mean values color-coded by dataset.

value added or removed by interpolation and elevation adjustment.

a. Burlington and Mt. Mansfield

Figures 4 and 5 show the daily probability distributions of station observations, Maurer et al. (2002) gridded observations, BCCA, BCCA-I, and BCCA-IA for maximum surface temperature, minimum surface temperature, and precipitation at Burlington and Mt. Mansfield. Results are presented for the best-performing BCCA ensemble member as described above by variable, IPSL-CM5A-LR for maximum and minimum surface temperature, and MPI-ESM-LR for precipitation.

Overall the differences between BCCA-IA and BCCA are relatively small at Burlington (Fig. 4), which is a result of the nearest BCCA grid cell being only 20 m higher than the Burlington station. BCCA-I reduces the average warm bias in BCCA maximum and minimum surface temperature, though this improvement is relatively small. BCCA-IA mean average maximum and minimum surface temperatures are practically unchanged from BCCA, a result of interpolation reducing the bias and the elevation adjustment enhancing it. The surface temperature elevation adjustment is uniform across all days, which effectively shifts the histogram. Therefore, the differences between BCCA-IA and BCCA histograms (not shown) depend on the degree to

which the histogram shifts and the values of adjacent bins and are largely inconsistent in sign and magnitude across the surface temperature range. Mean precipitation at Burlington is slightly improved in both BCCA-I and BCCA-IA relative to BCCA. BCCA contains a dry bias, interpolation alone (BCCA-I) increases average precipitation, and then the elevation adjustment (BCCA-IA) decreases the amount of precipitation because the coarse BCCA grid cell is higher (119 m) than the high-resolution BCCA-IA grid cell (99 m). As with surface temperature the elevation adjustment is small, but unlike surface temperature the elevation adjustment is dependent on the initial value of precipitation and is therefore not equal across the histogram. At Burlington BCCA-IA reduces the frequency of dry days and very small precipitation events ($0\text{--}1\text{ mm day}^{-1}$) and increases the frequency of most all other precipitation events (not shown).

In contrast to Burlington, the difference in elevation between the Mt. Mansfield station and the nearest BCCA grid cell is large, 560 m. Therefore, the elevation adjustment substantially decreases surface temperature and increases precipitation, and the relative effect of interpolation is small. Gridded observations, BCCA, BCCA-I, and BCCA-IA all overestimate surface temperature at Mt. Mansfield (Figs. 5a,b). This average overestimation of maximum surface temperature and minimum surface temperature in BCCA-IA is reduced

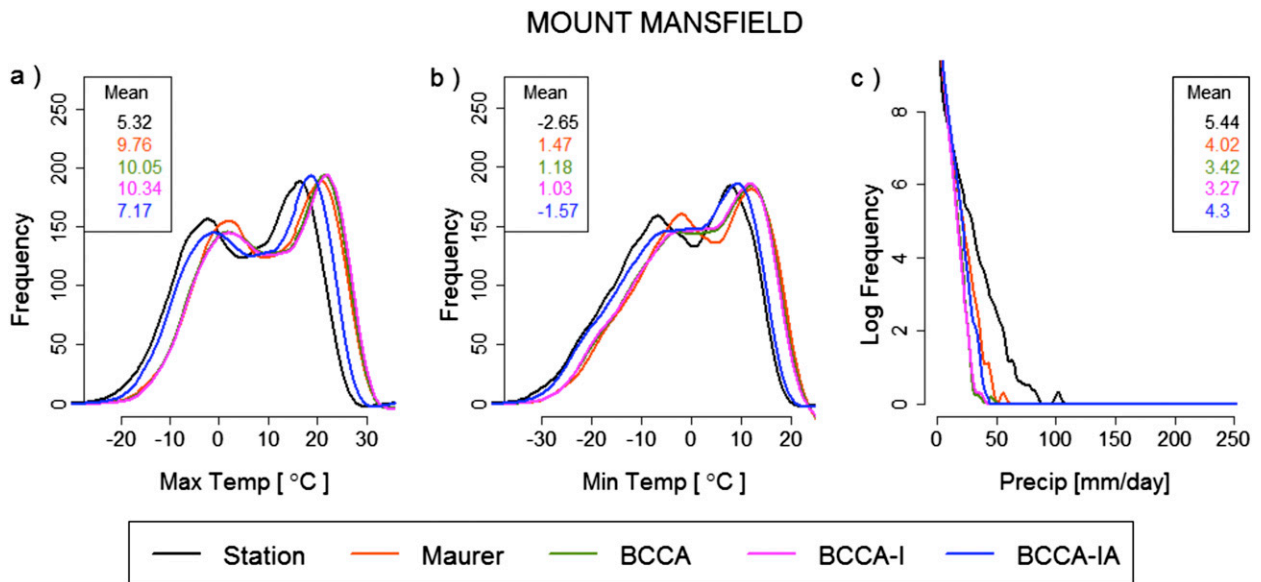


FIG. 5. As in Fig. 4, but for Mt. Mansfield station 1970–99.

by 2.88° and 2.75°C , respectively, relative to BCCA. In both cases, the elevation adjustment clearly adds value to the dataset when compared to BCCA or BCCA-I. Precipitation at Mt. Mansfield is also better reproduced on average by BCCA-IA, with the elevation adjustment process adding precipitation, resulting in a reduction of the dry bias in BCCA by 0.88 mm day^{-1} . In this case interpolation alone exacerbates the underestimation of precipitation by BCCA. While BCCA-IA precipitation is markedly improved from BCCA on average, the distribution of precipitation still contains significant inaccuracies, with the number of no- and low-precipitation days being too low and not improved by the elevation adjustment.

b. Elevation analysis

As topographic downscaling is a function of elevation, we explore the value added or removed by BCCA-IA relative to BCCA for all stations in the domain across elevation. In this analysis, we explicitly assess the full probability distribution of maximum surface temperature, minimum surface temperature, and precipitation using mean absolute bias, S_{score} , and RMSD. Figures 6, 7, and 8 show the difference between BCCA-IA and BCCA, and BCCA-I and BCCA, for mean absolute bias, S_{score} , and RMSD, relative to station observations, across the three variables and three ensemble members. Improvements in reproducing the observed histogram are by definition positive differences for S_{score} and negative differences for absolute bias and RMSD.

Reductions in maximum surface temperature absolute bias generally increase with increasing elevation

(Fig. 6a). Examining the overlap of the histograms using S_{score} , above 500 m BCCA-IA maximum surface temperature is generally closer to observations than BCCA (Fig. 6b). For Lake Placid, New York (591 m), and Pinkham Notch, New Hampshire (612 m), interpolation only and interpolation and elevation adjustment both add value to BCCA. For Mt. Mansfield and Mt. Washington (1909 m) interpolation only reduces S_{score} , but interpolation and elevation adjustment significantly increase S_{score} . At all four of these stations, improvements are well above the BCCA S_{score} ensemble spread, and also in excess of the 0.03 significance threshold described above. These findings are supported by the RMSD results, which like S_{score} show the benefits of topographic downscaling above 500 m (Fig. 6c). Below 500 m relatively smaller changes are found in BCCA-IA and BCCA-I, with the sign of the change (i.e., whether value is added or removed) depending on the station. In the context of the analysis above, we note that while Burlington is not the exception, it is also not the rule. Whether value is added or removed by topographic downscaling depends on the direction of the bias in the BCCA ensemble member combined with both the effects of interpolation and the elevation adjustment. We could have picked a BCCA ensemble member and station for which BCCA-IA performed better than BCCA. However, as the removed value at Burlington was relatively small, so would have been the added value, generally less than the spread of S_{score} or RMSD across BCCA ensemble members.

Qualitatively, the differences in BCCA-IA and BCCA minimum surface temperature are similar to the

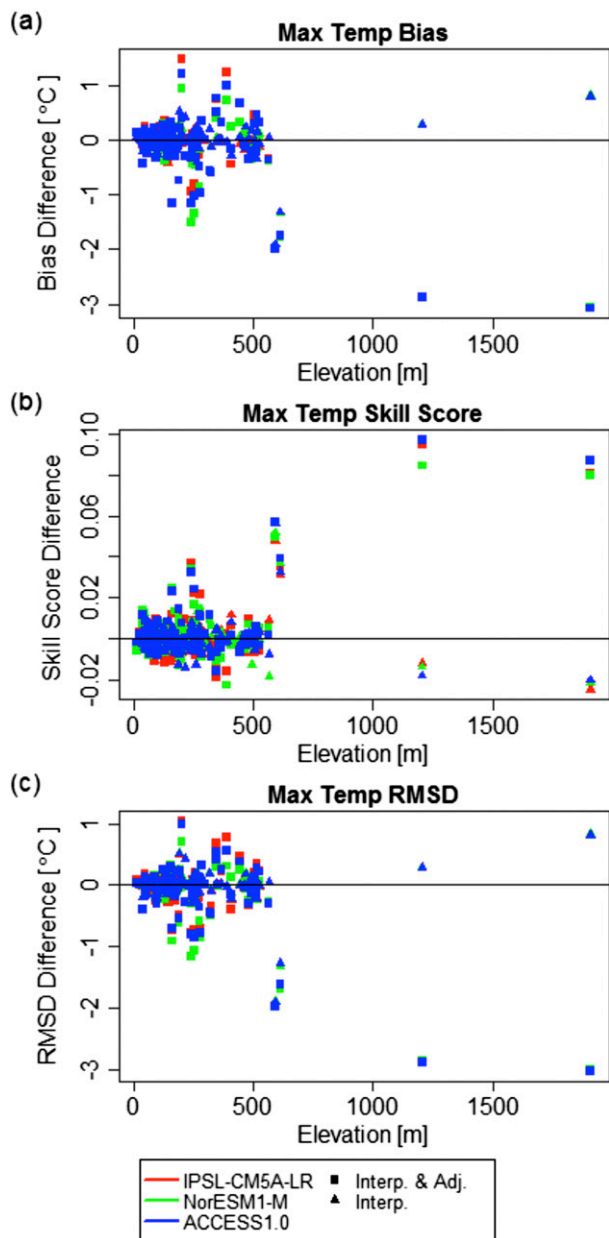


FIG. 6. Difference between BCCA-IA and BCCA, and BCCA-I and BCCA, daily max surface temperature: (a) mean absolute bias, (b) S_{score} , and (c) RMSD for all stations in the domain displayed by elevation 1970–99.

differences between BCCA-IA and BCCA maximum surface temperature. The absolute bias of BCCA-IA is generally reduced with increasing elevation (Fig. 7a). Below 500 m, S_{score} adjustments are relatively small and value is as likely to be added or removed from a station depending on the initial bias of the BCCA product (Fig. 7b). As with maximum surface temperature, for the stations above 500 m, including Lake Placid, Mt. Mansfield, and Mt. Washington, BCCA-IA generally

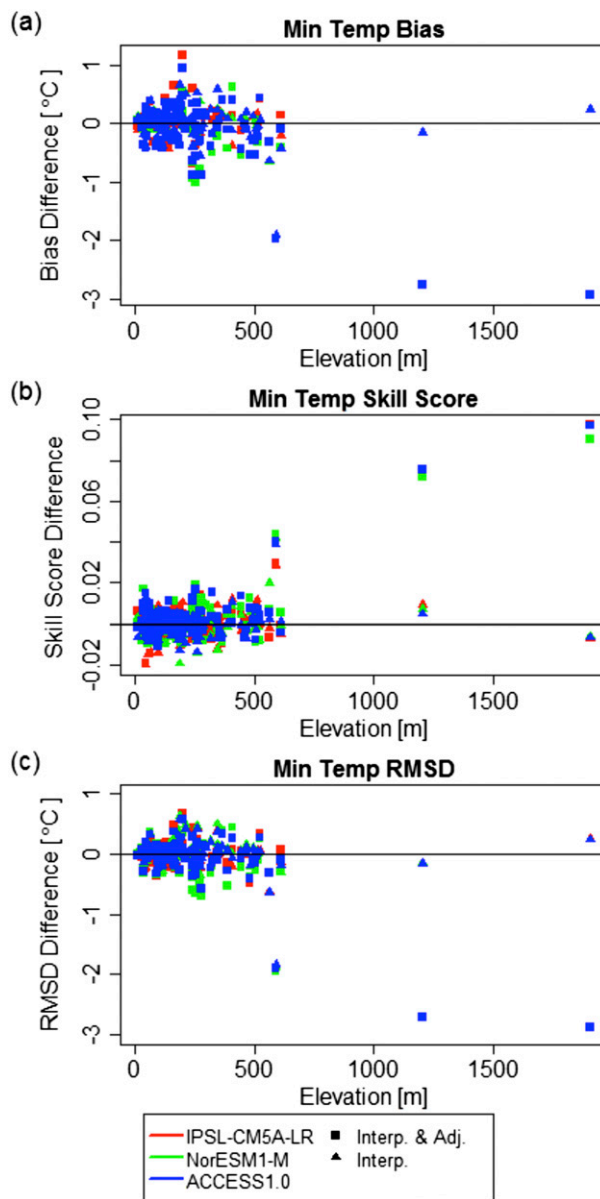


FIG. 7. As in Fig. 6, but for daily min surface temperature.

contains improvements in S_{score} over BCCA. RMSD corroborates the relatively small changes below 500 m and more consistent and significant changes above 500 m (Fig. 7c).

Overall, topographic downscaling reduces the mean absolute bias of BCCA precipitation (Fig. 8a), but when assessed using the probability distribution, BCCA-IA reduces the S_{score} (Fig. 8b) and increases the RMSD (Fig. 8c) at most stations across the domain. In many cases, BCCA-I also contains a reduction in S_{score} relative to BCCA, suggesting that the smoothing associated with interpolation is responsible for some of the removed value. There are a number of stations that have a large

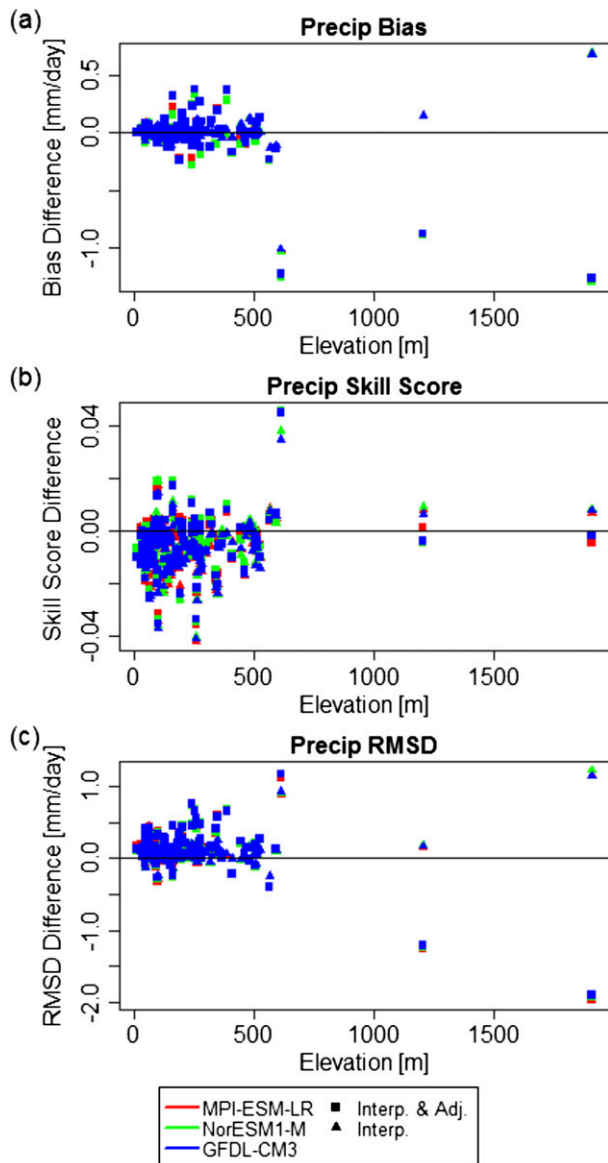


FIG. 8. As in Fig. 6, but for daily precipitation.

reduction in S_{score} relative to the BCCA ensemble range, and at two stations (Burlington, Vermont, and Coaticook, Canada) S_{score} is reduced in excess of the 0.03 significance threshold. RMSD is also degraded in BCCA-IA and BCCA-I relative to BCCA. However, while both S_{score} and RMSD yield the same general conclusions, there are some differences by station resulting from assessing frequency space (S_{score}), which is not weighted by precipitation amount, and the physical variable space (RMSD), which is informed by the magnitude of the precipitation deviation amounts. For example, BCCA-IA for Mt. Mansfield and Mt. Washington show negligible changes in S_{score} , but relatively large reductions in RMSD. Physically, there are two reasons that seem to

be causing degraded S_{score} and RMSD in BCCA-IA. On average, BCCA underestimates dry days and very small precipitation events ($0\text{--}1\text{ mm day}^{-1}$) and overestimates small precipitation events ($1\text{--}5\text{ mm day}^{-1}$). Interpolation exacerbates these biases by averaging across the nine nearest neighbors, which smooths the signal spatially. Unlike surface temperature, precipitation is highly spatially heterogeneous; thus, the smoothing creates more small precipitation events. Second, BCCA generally has a dry bias across the domain (not shown). Therefore, as precipitation is added by the elevation adjustment, more events are pushed out of the $0\text{--}1\text{ mm day}^{-1}$ bin to the $1\text{--}5\text{ mm day}^{-1}$ bin.

c. Domain-averaged performance

Tables 1–3 describe the mean absolute bias, S_{score} , and RMSD for maximum surface temperature, minimum surface temperature, and precipitation, respectively, averaged across all stations in the domain. Specifically, for each station and variable all three metrics were calculated and then averaged across the 98 stations in the domain. Maximum surface temperature mean absolute bias is reduced in both BCCA-IA and BCCA-I relative to BCCA (Table 1). While the improvement in mean absolute bias in BCCA-I is less than the spread across GCMs, the elevation adjustment reduces the mean absolute bias in maximum surface temperature by 16%–32%, depending on the GCM. The changes in S_{score} between BCCA-IA and BCCA maximum surface temperature for each ensemble member are slightly larger than the spread of S_{score} values across BCCA ensemble members, but remain well below the 0.03 significance threshold. The increases in S_{score} are likely a result of the bias reduction; however, they are modest as the bias of BCCA is low and errors in the shape of the probability distribution are not well addressed by interpolation or elevation adjustment. RMSD is reduced by interpolation and elevation adjustment by 13%–20% across the three BCCA ensemble members. This reduction for BCCA-IA relative to BCCA is much larger than the range of BCCA RMSD.

The value added to minimum surface temperature is similar to that of maximum surface temperature (Table 2). Minimum surface temperature mean absolute bias is reduced by both interpolation alone and interpolation and elevation adjustment. BCCA-IA minimum surface temperature mean absolute bias is 12%–22% less than BCCA minimum surface temperature mean absolute bias. While this reduction in mean absolute bias is less than that of maximum mean temperature, it is large compared to differences in mean absolute bias across BCCA ensemble members. Minimum surface temperature changes in S_{score} across BCCA-IA and BCCA are positive but

TABLE 1. Max surface temperature mean absolute bias, S_{score} , and RMSD averaged across all 98 stations in the domain for BCCA, BCCA-I, and BCCA-IA 1970–99.

	BCCA	Interpolation	Interpolation and adjustment
Mean bias (°C)			
IPSL-CM5A-LR	0.611	0.587	0.511
NorESM1-M	0.588	0.580	0.400
ACCESS1.0	0.573	0.554	0.435
S_{score}			
IPSL-CM5A-LR	0.863	0.863	0.866
NorESM1-M	0.860	0.860	0.864
ACCESS1.0	0.861	0.861	0.865
RMSD (°C)			
IPSL-CM5A-LR	0.804	0.790	0.702
NorESM1-M	0.801	0.804	0.641
ACCESS1.0	0.806	0.802	0.685

TABLE 2. Min surface temperature mean absolute bias, S_{score} , and RMSD averaged across all 98 stations in the domain for BCCA, BCCA-I, and BCCA-IA 1970–99.

	BCCA	Interpolation	Interpolation and adjustment
Mean bias (°C)			
IPSL-CM5A-LR	0.604	0.578	0.534
NorESM1-M	0.616	0.609	0.478
ACCESS1.0	0.591	0.573	0.490
S_{score}			
IPSL-CM5A-LR	0.859	0.859	0.861
NorESM1-M	0.858	0.858	0.861
ACCESS1.0	0.855	0.854	0.858
RMSD (°C)			
IPSL-CM5A-LR	0.871	0.863	0.805
NorESM1-M	0.855	0.868	0.751
ACCESS1.0	0.990	0.994	0.916

much smaller than the 0.03 threshold, and the differences between BCCA-IA and BCCA are slightly less than the range of BCCA S_{score} . Consistent with changes in mean absolute bias and S_{score} , RMSD decreases from BCCA to BCCA-I to BCCA-IA, with overall reductions in RMSD between BCCA-IA and BCCA of 7%–12%.

Unlike surface temperature, the mean absolute bias, S_{score} , and RMSD qualitatively differ on whether value is added or subtracted to precipitation by interpolation and adjustment (Table 3). Precipitation mean absolute bias in BCCA-IA is reduced by 7%–15% relative to BCCA. This reduction in mean absolute is somewhat less than the difference in mean absolute bias across BCCA ensemble members. There is little reduction in the mean absolute bias of BCCA by interpolation only, showing minimal value of BCCA-I for precipitation in this domain. Changes in S_{score} between BCCA-IA and BCCA are negative, suggesting degraded performance in BCCA-IA, and larger than the BCCA ensemble spread of S_{score} ; however, they are well below the 0.03 significance threshold. The increase in RMSD between BCCA-IA and BCCA is 6% for all BCCA-IA ensemble members. Similar increases in BCCA RMSD are found in BCCA-I, suggesting that, as described above, this degradation of performance is primarily a result of smoothing associated with interpolation. Smoothing reduces the tails of the probability distribution (dry days and large precipitation events) and overall variability spatially, which are generally more pronounced in observations, thus decreasing S_{score} and increasing RMSD. We note that mean absolute bias is not as strongly dependent on the distribution of daily precipitation as S_{score} and RMSD, and thus the reduction in mean absolute bias from the elevation adjustment is dominant.

Figure 9 explores the relationship between the absolute bias correction applied, or BCCA-IA absolute bias

minus BCCA absolute bias, the original absolute bias of BCCA, and the change in elevation between the 30'' BCCA-IA and 1/8° BCCA. Across maximum surface temperature, minimum surface temperature, and precipitation a consistent pattern emerges. As the initial bias in BCCA increases, the ability of topographic downscaling to reduce that bias also increases. For absolute biases above approximately 1°C for maximum and minimum surface temperatures, and 0.25 mm day⁻¹ for precipitation, topographic downscaling starts consistently adding value. Figure 9, along with Figs. 6–8, shows that either a large bias in BCCA or an increasing elevation delta can result in the topographic downscaling value added. When stations have both a large initial bias in the correct direction (i.e., counter to the adjustment) and a difference in elevation between BCCA-IA and BCCA that is greater than 200m, topographic downscaling often results in a substantial reduction of

TABLE 3. Precipitation mean absolute bias, S_{score} , and RMSD averaged across all 98 stations in the domain for BCCA, BCCA-I, and BCCA-IA 1970–99.

	BCCA	Interpolation	Interpolation and adjustment
Mean bias (mm day ⁻¹)			
MPI-ESM-LR	0.189	0.184	0.166
NorESM1-M	0.183	0.181	0.155
GFDL CM3	0.216	0.208	0.200
S_{score}			
MPI-ESM-LR	0.833	0.826	0.828
NorESM1-M	0.831	0.825	0.827
GFDL CM3	0.829	0.822	0.824
RMSD (mm day ⁻¹)			
MPI-ESM-LR	2.007	2.104	2.137
NorESM1-M	2.022	2.119	2.149
GFDL CM3	2.140	2.237	2.270

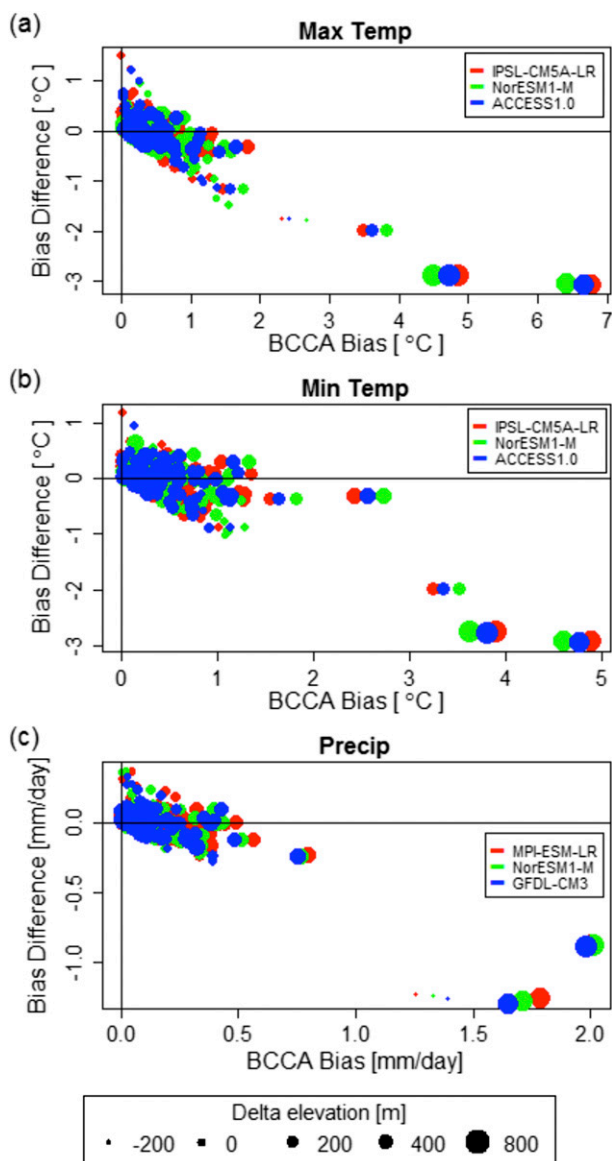


FIG. 9. Mean absolute bias removed (negative bias difference) or added (positive bias difference) by topographic downscaling compared to the original BCCA bias: (a) max surface temperature, (b) min surface temperature, and (c) precipitation for all stations in the domain 1970–99. The change in elevation between the 30'' BCCA-IA and 1/8° BCCA grid cell is denoted by the size of the point.

absolute bias. For stations with low bias at low elevations, the change in absolute bias is generally small and can be either positive or negative.

4. Conclusions

In this manuscript, we develop a methodology for topographically downscaling intermediately downsampled data (1/8°) to 30''. We apply this methodology over the mountainous Northeast to explore the added value of

topographic downscaling. We find that topographic downscaling has benefits in some situations (defined by variables and elevations). BCCA absolute bias is noisy at low elevations, with BCCA as likely to underpredict or overpredict surface temperature or precipitation with no clear relationship to topography. Thus, noise dominates any elevation adjustment. For example, the elevation difference between the 30'' and 1/8° DEM at the Burlington station, 20 m, is as likely to exacerbate the bias in the BCCA product as it is to ameliorate it, though regardless of direction, the change will be small. As the elevation difference increases, however, the topographic downscaling adjustment begins to dominate this noise and is likely to add value. For example, Mt. Mansfield elevation adjustments are large, and the improvements from topographic downscaling to BCCA maximum and minimum surface temperature are clear.

Therefore, we find that the utility of topographic downscaling depends on two quantities: the magnitude and direction of the BCCA bias—specifically, a relatively large bias that is consistent with the coarse topography of BCCA—and the elevation difference—specifically, a large enough difference in elevation between 30'' and 1/8° DEMs to apply a substantial correction. We find relatively large biases consistent with coarse topography and elevation differences most often at elevations above 500 m. Averaged across the domain, topographic downscaling reduces the absolute bias for maximum surface temperature, minimum surface temperature, and precipitation. This overall value added shows that the signal dominates the noise in aggregate for our domain. We expect that in areas with greater topographic relief the value of this methodology will be more pronounced.

We have attempted to develop a downscaling method that addresses the rich spatial variation of the region and yet is also generalizable, leveraging only empirical relationships between topography and surface temperature and precipitation. We note that our study uses BCCA, which is based on climate analogs. Alternate methods of downscaling could lead to different behavior at high resolutions. Further, we note that our empirical relationships are based on historical data; thus, care must be taken when applying this downscaling methodology to future climate. For example, expected changes in the capacity of the atmosphere to hold moisture could alter both surface temperature and precipitation elevation adjustments. Also, we note that results were not tested for sensitivity to interpolation method, which contributes to the net effect of topographic downscaling, especially at low elevations.

Future work will explore how land–atmosphere interactions within Lake Champlain basin could inform

high-resolution downscaling and alternate methods of further bias correction. Examples include precipitation distributions associated with mountain aspect and dominant winds and an additional layer of bias correction based on station data. Finally, as this dataset is specifically developed for climate impacts applications, testing whether topographic downscaling or alternate methods of downscaling add value to climate impacts assessments is vital to the motivation of this research.

Acknowledgments. This work was supported by the Vermont Experimental Program for Stimulating Competitive Research (NSF Award EPS-1101317). Many thanks to Levi Brekke, Ed Maurer, and Tom Pruitt for their assistance with BCCA data, as well as Alan Betts for his valuable ideas and insights. We acknowledge the World Climate Research Programme's Working Group on Coupled Modelling, which is responsible for CMIP, and we thank the climate modeling groups for producing and making available their model output. For CMIP the U.S. Department of Energy's Program for Climate Model Diagnosis and Intercomparison provides coordinating support and led development of software infrastructure in partnership with the Global Organization for Earth System Science Portals. Further, we acknowledge high-performance computing support from Yellowstone (ark:/85065/d7wd3xhc) provided by NCAR's Computational and Information Systems Laboratory, sponsored by the National Science Foundation.

REFERENCES

- Abatzoglou, J. T., and T. J. Brown, 2012: A comparison of statistical downscaling methods suited for wildfire applications. *Int. J. Climatol.*, **32**, 772–780, doi:10.1002/joc.2312.
- Ahmed, K. F., G. Wang, J. Silander, A. M. Wilson, J. M. Allen, R. Horton, and R. Anyah, 2013: Statistical downscaling and bias correction of climate model outputs for climate change impact assessment in the U.S. Northeast. *Global Planet. Change*, **100**, 320–332, doi:10.1016/j.gloplacha.2012.11.003.
- Barry, R. G., 2008: *Mountain Weather and Climate*. 3rd ed. Routledge, 512 pp.
- Blandford, T. R., K. S. Humes, B. J. Harshburger, B. C. Moore, V. P. Walden, and H. Ye, 2008: Seasonal and synoptic variations in near-surface air temperature lapse rates in a mountainous basin. *J. Appl. Meteor. Climatol.*, **47**, 249–261, doi:10.1175/2007JAMC1565.1.
- Brekke, L., B. Thrasher, E. P. Maurer, and T. Pruitt, 2013: Downscaled CMIP3 and CMIP5 climate projections: Release of downscaled CMIP5 climate projections, comparison with preceding information, and summary of user needs. USBR Tech. Memo., 104 pp. [Available online at http://gdo-dcp.ucllnl.org/downscaled_cmip_projections/techmemo/downscaled_climate.pdf]
- Daly, C., G. H. Taylor, W. P. Gibson, T. W. Parzybok, G. L. Johnson, and P. A. Pasteris, 2000: High-quality spatial climate data sets for the United States and beyond. *Trans. Amer. Soc. Agric. Biol. Eng.*, **43**, 1957–1962, doi:10.13031/2013.3101.
- Dudhia, J., 1993: A nonhydrostatic version of the Penn State–NCAR mesoscale model: Validation tests and simulation of an Atlantic cyclone and cold front. *Mon. Wea. Rev.*, **121**, 1493–1513, doi:10.1175/1520-0493(1993)121<1493:ANVOTP>2.0.CO;2.
- Giorgi, F., C. Jones, and G. R. Asrar, 2009: Addressing climate information needs at the regional level: The CORDEX framework. *WMO Bull.*, **58** (3), 175–183. [Available online at http://www.wmo.int/pages/publications/bulletinarchive/archive/58_3_en/documents/58_3_giorgi_en.pdf.]
- Guilbert, J., B. Beckage, J. M. Winter, R. M. Horton, T. Perkins, and A. Bombles, 2014: Impacts of projected climate change over the Lake Champlain basin in Vermont. *J. Appl. Meteor. Climatol.*, **53**, 1861–1875, doi:10.1175/JAMC-D-13-0338.1.
- Hartkamp, A. D., K. De Beurs, A. Stein, and J. W. White, 1999: Interpolation techniques for climate variables. Rep. NRG-GIS 99-01, CIMMYT, 26 pp.
- Hidalgo, H. G., M. D. Dettinger, and D. R. Cayan, 2008: Downscaling with constructed analogues: Daily precipitation and temperature fields over the United States. California Energy Commission PIER Final Project Rep. CEC-500-2007-123, 48 pp. [Available online at <http://www.energy.ca.gov/2007publications/CEC-500-2007-123/CEC-500-2007-123.PDF>.]
- Hijmans, R. J., S. E. Cameron, J. L. Parra, P. G. Jones, and A. Jarvis, 2005: Very high resolution interpolated climate surfaces for global land areas. *Int. J. Climatol.*, **25**, 1965–1978, doi:10.1002/joc.1276.
- Huntington, J. L., and R. G. Niswonger, 2012: Role of surface-water and groundwater interactions on projected summertime streamflow in snow dominated regions: An integrated modeling approach. *Water Resour. Res.*, **48**, W11524, doi:10.1029/2012WR012319.
- Islam, A., L. R. Ahuja, L. A. Garcia, L. Ma, A. S. Saseendran, and T. J. Trout, 2012: Modeling the impacts of climate change on irrigated corn production in the central Great Plains. *Agric. Water Manage.*, **110**, 94–108, doi:10.1016/j.agwat.2012.04.004.
- Li, J., and A. D. Heap, 2014: Spatial interpolation methods applied in the environmental sciences: A review. *Environ. Modell. Software*, **53**, 173–189, doi:10.1016/j.envsoft.2013.12.008.
- Liston, G. E., and K. Elder, 2006: A meteorological distribution system for high-resolution terrestrial modeling (MicroMet). *J. Hydrometeorol.*, **7**, 217–234, doi:10.1175/JHM486.1.
- Livneh, B., E. A. Rosenberg, C. Lin, B. Nijssen, V. Mishra, K. M. Andreadis, E. P. Maurer, and D. P. Lettenmaier, 2013: A long-term hydrologically based dataset of land surface fluxes and states for the conterminous United States: Update and extensions. *J. Climate*, **26**, 9384–9392, doi:10.1175/JCLI-D-12-00508.1.
- Lloyd, C. D., 2005: Assessing the effect of integrating elevation data into the estimation of monthly precipitation in Great Britain. *J. Hydrol.*, **308**, 128–150, doi:10.1016/j.jhydrol.2004.10.026.
- Maurer, E. P., and H. G. Hidalgo, 2008: Utility of daily vs. monthly large-scale climate data: An intercomparison of two statistical downscaling methods. *Hydrol. Earth Syst. Sci.*, **12**, 551–563, doi:10.5194/hess-12-551-2008.
- , A. W. Wood, J. C. Adam, D. P. Lettenmaier, and B. Nijssen, 2002: A long-term hydrologically based dataset of land surface fluxes and states for the conterminous United States. *J. Climate*, **15**, 3237–3251, doi:10.1175/1520-0442(2002)015<3237:ALTHBD>2.0.CO;2.
- , H. G. Hidalgo, T. Das, M. D. Dettinger, and D. R. Cayan, 2010: The utility of daily large-scale climate data in the

- assessment of climate change impacts on daily streamflow in California. *Hydrol. Earth Syst. Sci.*, **14**, 1125–1138, doi:10.5194/hess-14-1125-2010.
- Mearns, L. O., W. Gutowski, R. Jones, R. Leung, S. McGinnis, A. Nunes, and Y. Qian, 2009: A regional climate change assessment program for North America. *Eos, Trans. Amer. Geophys. Union*, **90**, 311–311, doi:10.1029/2009EO360002.
- Menne, M. J., and Coauthors, 2012: Global Historical Climatology Network—Daily, version 3.21. Subset used: GHCN-Daily, NOAA/NCDC, accessed 15 June 2015, doi:10.7289/V5D21VHZ.
- Moss, R. H., and Coauthors, 2010: The next generation of scenarios for climate change research and assessment. *Nature*, **463**, 747–756, doi:10.1038/nature08823.
- Nakićenović, N., and R. Swart, Eds., 2000: *Special Report on Emissions Scenarios*. Cambridge University Press, 570 pp.
- Norton, C. W., P.-S. Chu, and T. A. Schroeder, 2011: Projecting changes in future heavy rainfall events for Oahu, Hawaii: A statistical downscaling approach. *J. Geophys. Res.*, **116**, D17110, doi:10.1029/2011JD015641.
- Perkins, S. E., A. J. Pitman, N. J. Holbrook, and J. McAneney, 2007: Evaluation of the AR4 climate models' simulated daily maximum temperature, minimum temperature, and precipitation over Australia using probability density functions. *J. Climate*, **20**, 4356–4376, doi:10.1175/JCLI4253.1.
- Petkova, E. P., R. M. Horton, D. A. Bader, and P. L. Kinney, 2013: Projected heat-related mortality in the US urban northeast. *Int. J. Environ. Res. Public Health*, **10**, 6734–6747, doi:10.3390/ijerph10126734.
- Pierce, D. W., and Coauthors, 2013: Probabilistic estimates of future changes in California temperature and precipitation using statistical and dynamical downscaling. *Climate Dyn.*, **40**, 839–856, doi:10.1007/s00382-012-1337-9.
- PRISM Climate Group, 2014: PRISM climate data. Oregon State University, accessed 15 October 2014. [Available online at <http://prism.oregonstate.edu>.]
- Rajagopal, S., F. Dominguez, H. V. Gupta, P. A. Troch, and C. L. Castro, 2014: Physical mechanisms related to climate-induced drying of two semiarid watersheds in the southwestern United States. *J. Hydrometeor.*, **15**, 1404–1418, doi:10.1175/JHM-D-13-0106.1.
- Rolland, C., 2003: Spatial and seasonal variations of air temperature lapse rates in alpine regions. *J. Climate*, **16**, 1032–1046, doi:10.1175/1520-0442(2003)016<1032:SASVOA>2.0.CO;2.
- Rosenzweig, C., and Coauthors, 2014: Assessing agricultural risks of climate change in the 21st century in a global gridded crop model intercomparison. *Proc. Natl. Acad. Sci. USA*, **111**, 3268–3273, doi:10.1073/pnas.1222463110.
- Sunyer, M. A., H. Madsen, and P. H. Ang, 2012: A comparison of different regional climate models and statistical downscaling methods for extreme rainfall estimation under climate change. *Atmos. Res.*, **103**, 119–128, doi:10.1016/j.atmosres.2011.06.011.
- Taylor, K. E., R. J. Stouffer, and G. A. Meehl, 2012: An overview of CMIP5 and the experiment design. *Bull. Amer. Meteor. Soc.*, **93**, 485–498, doi:10.1175/BAMS-D-11-00094.1.
- Thornton, P. E., S. W. Running, and M. A. White, 1997: Generating surfaces of daily meteorological variables over large regions of complex terrain. *J. Hydrol.*, **190**, 214–251, doi:10.1016/S0022-1694(96)03128-9.
- van der Linden, P., and J. F. B. Mitchell, Eds., 2009: ENSEMBLES: Climate change and its impacts: Summary of research and results from the ENSEMBLES project. ENSEMBLES Rep., Met Office Hadley Centre, 160 pp. [Available online at http://ensembles-eu.metoffice.com/docs/Ensembles_final_report_Nov09.pdf.]
- Westerling, A. L., and B. P. Bryant, 2008: Climate change and wildfire in California. *Climatic Change*, **87**, 231–249, doi:10.1007/s10584-007-9363-z.
- Wilby, R. L., T. M. L. Wigley, D. Conway, P. D. Jones, B. C. Hewitson, J. Main, and D. S. Wilks, 1998: Statistical downscaling of general circulation model output: A comparison of methods. *Water Resour. Res.*, **34**, 2995–3008, doi:10.1029/98WR02577.
- Wood, A. W., L. R. Leung, V. Sridhar, and D. P. Lettenmaier, 2004: Hydrologic implications of dynamical and statistical approaches to downscaling climate model outputs. *Climatic Change*, **62**, 189–216, doi:10.1023/B:CLIM.0000013685.99609.9e.